DOI: 10.36959/942/335 | Volume 1 | Issue 1

Journal of Physical Medicine

Original Article Open Access

Functional MRI Reveals Emotional Modulation of Pain Processing in the Human Cervical Spinal Cord and Brainstem

Theresa A McIver[1], Jennifer Kornelsen[2] and Patrick W Stroman[1*]

[1]*Centre for Neuroscience Studies, Queen's University, Kingston, Ontario, Canada*

[2]*Department of Radiology, University of Manitoba, Winnipeg, Manitoba, Canada*

Abstract

Background: Prior research has demonstrated that emotional state can influence pain perception. If a noxious stimulus is coupled with a negative emotional stimulus, the perception of the noxious stimulus will be heightened by the aversive associations of the negative emotional stimulus. In contrast, pain ratings decrease with positive emotional influence. The aim of the current study was to characterize the emotional modulation of pain processing in the spinal cord and brainstem using functional MRI.

Methods: Twenty-one healthy, right-handed females, aged 18-30 (*M age* = 21.5) underwent an fMRI scan of the spinal cord and brainstem while completing a heat pain-rating task. Participants received noxious thermal stimulus to the thenar eminence of the right hand while viewing images of varying emotional contexts (Positive, Neutral, or Negative), and provided ratings of pain Intensity and Unpleasantness.

Results: Pain ratings reflected a significant effect for emotional context, with the Negative emotional condition eliciting significantly greater pain Intensity (M = 48.74, SD = 10.60) and Unpleasantness (M = 36.60, SD = 11.92) ratings than the Positive Intensity (M = 44.22, SD = 10.75) and Unpleasantness (M = 29.05, SD = 10.09) ratings ($p < 0.01$). In addition to replicating the well-established effect for emotional modulation of pain perception, BOLD responses in regions of the spinal cord and brainstem that are known to function in pain processing also exhibited an effect for descending emotional modulation of pain processing. These regions included the ipsilateral, dorsal horn of the T1 spinal cord segment (caudal to the segment corresponding to the stimulated dermatome), as well as regions in the brainstem approximating the dorsal reticular nucleus of the caudal medulla and the parabrachial nuclei of the pons ($p < 0.001$).

Conclusion: These findings provide novel insight into the neural correlates of descending emotional modulation of pain processing. Furthermore, this study highlights key areas of focus for future research to examine potential individual-level differences in emotional modulation of pain neural processing in the spinal cord and brainstem.

Keywords

Emotional Modulation of Pain, fMRI, Spinal cord, Brainstem

Introduction

Emotions influence pain perception, however the neural mechanisms involved in this modulatory process are not fully understood. According to Motivational Priming Theory [1], emotional responses elicited by different environmental triggers modulate our reaction to those triggers by activating either an aversive/defensive or appetitive drive [2]. This theory has been studied in the context of priming for motor responses, with results consistently demonstrating that emotional stimuli lead to enhanced preparedness to perform motor actions in response to emotionally-charged stimuli [3-7]. This emotional priming for motor responses parallels similar priming for somatosensory stimuli such as pain. If a noxious stimulus is coupled with a negative emotional stimulus (for example: odors [3], emotional sentences [4],

***Corresponding author:** Patrick W Stroman, Centre for Neuroscience Studies, Queen's University, 2nd floor, Botterell Hall, 18 Stuart Street, K7L 3N6, Kingston, Ontario, Canada, Tel: 1-613-533-3245, Fax: 1-613-533-6840

Accepted: August 27, 2018; **Published online:** August 29, 2018

Citation: McIver TA, Kornelsen J, Stroman PW (2018) Functional MRI Reveals Emotional Modulation of Pain Processing in the Human Cervical Spinal Cord and Brainstem. J Phys Med 1(1):10-23

films [5], or pictures [6]), the perception of the noxious stimulus will be heightened by the aversive associations of the negative emotional stimulus [8]. Increased sensitization to the noxious stimulus can therefore facilitate faster withdrawal responses. In contrast, the reverse pattern has been shown for the influence of positive emotion [9].

To explore this effect more deeply, various physiological measures have been employed, including: Skin conductance responses [6,8], nociceptive flexion reflex (NFR) [1,9,10], brain event related potentials (ERPs) [11], positron emission tomography (PET) [12], and functional magnetic resonance imaging (fMRI) [13-15]. Although several techniques have been applied to study the underlying neural mechanisms in the brain, this provides an incomplete representation of how the central nervous system processes emotional modulation of pain. Subcortical neural mechanisms in both the brainstem and spinal cord play a critical role in descending modulation of pain. Therefore, an investigation of the subcortical neural response involved in emotional modulation of pain is essential to a comprehensive understanding of this phenomenon. The objective of this study is to use functional magnetic resonance imaging (fMRI) to identify the neural correlates of emotional modulation of pain in the brainstem and spinal cord in healthy individuals, comparing between the effects of positive, neutral, and negative affective manipulation. We hypothesize there are significant differences in blood oxygenation-level dependent (BOLD) responses between the three conditions in regions of both the spinal cord and brainstem involved in processing nociception. These differences reflect altered neural processing of nociceptive signals to produce the net pain response.

Methods

Participants

Participants included 21 healthy, right-handed females, aged 18-30 (M_{age} = 22) who completed all stages of the study. This is out of 32 participants originally recruited, with 11 participants not completing all study stages or failing to discriminate temperature variations. Females were recruited to avoid known sex differences in pain perception [16]. Study participation was limited to the luteal stage of the menstrual cycle (final 2 weeks of the natural cycle), or the final 2 weeks in the cycle of oral contraceptives, in order to eliminate potential variability in pain perception due to fluctuations in the hormone cycle [17]. As a measure of control for psychological state, participants completed questionnaires for depression (BDI-II) [18], anxiety (STAI) [19], social desirability (Crowne-Marlowe Social Desirability Scale) [20], and pain catastrophizing (PCS) [21]. All participants provided written, informed consent and this study was reviewed and approved by the institutional ethics board.

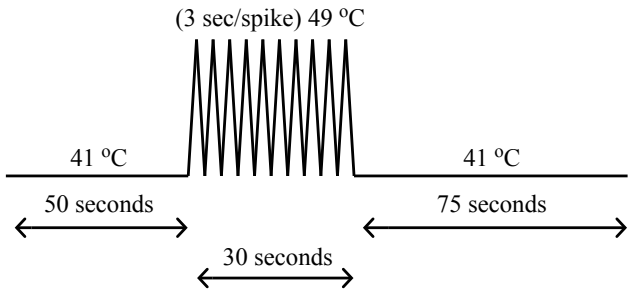

Figure 1: Thermal stimulation paradigm, with heat pulses presented at a frequency of 0.33 Hz. Every participant experienced heat pulse with amplitudes that peaked at a temperature that was 8 °C higher than baseline. Baseline temperature (shown here as 41 °C) and the peak temperature (shown here as 49 °C) were calibrated for each individual's pain sensitivity.

Noxious thermal stimulus

Noxious thermal stimulation was administered to the thenar eminence of the right hand (corresponding to the 6th cervical dermatome) via an MRI-compatible Medoc TSA-II thermal sensory analyzer (Medoc Ltd, Ramat Yishai, Israel). Stimulation was applied in a block-like design, with 2 baseline innocuous thermal sensory periods separated by a period of noxious (painful) thermal stimulation. The baseline innocuous temperature was set to 8°C below the noxious thermal temperature (determined as outlined in the Study Protocol). The period preceding noxious stimulation was 50 seconds, the post-stimulation period was 75 seconds, and the stimulation period consisted of 10 brief increases in temperature (heat pulses) over the course of 30 seconds (temperature peaks were presented every 3 seconds, 0.33 Hz) (Figure 1). The use of repeated heat pulses produces a more robust stimulation effect and corresponding BOLD responses than a constant stimulus, by avoiding habituation effects of receptors [22-25]. Each pulse consisted of an 8 °C increase from baseline over the course of 1.5 seconds, peaking at the pre-determined noxious temperature, followed by a return to baseline temperature over 1.5 seconds. There was a two-minute break between runs to avoid sensitization and allow nociceptors in the skin to recover [26].

Participants were asked to rate the noxious thermal stimulus using 0-100 pain rating scales for both pain Intensity and pain Unpleasantness [3,15,27]. The pain Intensity scale included verbal descriptors ranging from "no sensation" at 0, to "intolerable pain" at 100, and has been established in previous studies [28,29]. The pain Unpleasantness scale was a modified version of the pain Intensity scale. It similarly ranged from "neutral" at 0 to "intolerably unpleasant" at 100 in terms of numeric ratings.

Visual affective stimuli

The emotional stimuli consisted of images (546 total) selected for Positive, Neutral, and Negative valence, mostly from the International Affective Picture System (IAPS) (482 images) [30]. Due to an insufficient number of high arousal positive images in the IAPS, a portion of the positive images (64) were supplemented from the internet as a publicly available source. Supplemented images were rated in terms of both valence and arousal by a separate group of 28 women (aged 18-45) using the Self-Assessment Manikin (SAM). The SAM scale ranged from 1 = "negative" to 9 = "positive" for valence, and from 1 = "calm" to 9 = "excited" for arousal. Only images that rated consistently with those from the IAPS were included in the sample used in the Positive condition and had valence and arousal ratings of 5.70 ± 0.64 and 4.95 ± 0.43 (mean ± *s.d.*), respectively.

Positive images were selected to be high in valence, 6.55 ± 1.01, whereas negative images were selected for low valence, 2.28 ± 0.49, and neutral images were of medium valence, 4.94 ± 0.49. The images for the Positive and Negative conditions were both selected to be higher in arousal (Positive: 5.51 ± 0.77; Negative: 5.84 ± 0.76), while the neutral images were low arousal, 3.56 ± 0.63. All images were resized to the same dimensions (1024 × 768 pixels).

Study protocol

Training session: Phase I: Prior to the imaging session, all participants underwent a training session in a "sham" MRI environment, to familiarize them with the study procedures and reduce anxiety. Participants were asked to refrain from any drug use for two days prior to the study and confirmed their adherence in a screening form. The participant's overall comfort level was monitored throughout the experiment to ensure that they were not experiencing any incidental pain or discomfort, apart from the experimental stimulus. Training began with an explanation of the rating scales for pain Intensity and Unpleasantness as described by Price and colleagues [30]. Participants were taken through a sequential process of providing Intensity and Unpleasantness ratings first to single and then multiple heat pulses, over a range of temperatures. If a participant was able to accurately discriminate the difference in the temperature of the pulses from trial to trial, they progressed to a 10-pulse trial where they were asked to rate only the 10th pulse in the series, as they felt it occur. The temperature of the 10-pulse trials was adjusted until the participant consistently reported a pain Intensity rating of 50.

Training session: Phase II: If the participant passed the Phase I, they were positioned supine in the sham MRI complete with a replica head coil and mirror for viewing a rear-projection screen. The participant then experienced the 10-pulse heat pain paradigm in combination with visual affective stimuli which were presented on the screen. Participants were not informed that the noxious heat pulses for all remaining runs (trials) were set at the same temperature, as calibrated in Phase I. Throughout the entire time-course of each run, images of a set valence type (Positive, Neutral, or Negative) were presented on the screen (6 sec/picture, 26 pictures per run, with no image presented more than once). Participants completed three runs of each valence, resulting in nine runs total. The conditions were presented in a pseudo-randomized order across repeated runs with the restriction that a condition-type could not be repeated more than twice in a row. Participants were instructed to watch the images on the screen and to verbally rate the noxious stimulus on the 10th pulse, as they felt it occur, first in terms of pain Intensity, and then pain Unpleasantness. At the end of the run, the pain rating scales were presented on the screen and participants were asked to repeat their pain ratings, with the scale visible as a reference, and their ratings were recorded.

Functional MRI Session

Preparation

Imaging was carried out on a later day to avoid sensitization of the nociceptors in the skin or habituation to the emotional stimuli. Upon arrival for the imaging session, participants were reminded how to use the rating scales. Set-up for the imaging session closely followed that of the sham training. Participants were positioned supine on the bed of the MRI system and the thermode was fixed to the right thenar eminence. The head coil was positioned with a mirror attached to allow participants to view a rear-projection screen. Padding was used to ensure participant comfort and to reduce head/neck motion. Once the bed was moved inside the bore, participants performed several pain-rating practice trials to confirm the calibration of the temperature and to allow for subtle adjustments if needed.

FMRI Data acquisition

Imaging took place in a 3 Tesla, whole-body MRI system (Siemens Magnetom Trio; Siemens, Erlangen, Germany), at Queen's University, Kingston Ontario. Data were collected using a spine array-receiver coil and a posterior neck coil, with a body coil used for transmission of radiofrequency (RF) excitation pulses. Initial localizer images were acquired in 3 planes to guide subsequent slice positioning. FMRI data were acquired using a half-Fourier single-shot fast spin-echo (HASTE) for optimal image quality in the brainstem and spinal cord. Images were acquired in nine 2 mm thick contiguous sagittal slices, at a repetition time (TR) of 6.75 seconds per

volume (0.75 sec/slice). The echo time (TE) was set at 76 msec for optimal BOLD contrast in this region [31,32]. Each sagitttal slice spanned from the top of the corpus callosum to the T1/T2 intervertebral disc. Data were acquired with a 280 mm × 210 mm FOV and a matrix size of 192 × 144, providing a resolution of 1.5 mm × 1.5 mm × 2 mm. A spatial saturation pulse was applied anterior to the spine to reduce motion artifacts [33]. In total, there were 12 functional runs acquired, with four runs for each condition (Positive, Neutral, and Negative) and 23 volumes per run, resulting in 92 volumes per condition. The order of the conditions was randomized to avoid order effects and habituation to the emotional stimuli.

The combined pain and emotional modulation paradigm for fMRI runs was nearly identical to that used for "sham" training. Participants again experienced the 10-pulse paradigm, with the emotional images being presented throughout the duration of the run and were required to provide a verbal indication of pain Intensity and pain Unpleasantness rating for the 10th pulse, as they felt it happen. At the end of the run, participants repeated their ratings with the pain rating scales displayed on the screen as a reference. No emotional image was viewed more than once, so the images presented during the fMRI session were not the same as those during the training session, but they were matched in terms of the relative valence and arousal.

Data Analysis

Behavioral data

Pain ratings for each individual were combined across the sham training and the fMRI session. Descriptive statistics were calculated for the Positive, Neutral, and Negative conditions and the means of these conditions were compared using a repeated measures ANOVA, with follow-up pairwise comparisons, Bonferroni corrected for multiple comparisons.

Functional MRI data: preprocessing

Data were analyzed using custom-written software in MATLAB (MathWorks, Natick, MA). Data preprocessing included conversion to NifTI format, co-registration to correct for bulk motion, and spatial normalization to a pre-defined anatomical template. The details of the pre-processing methods are provided in Supplementary On-Line Material and have been extensively validated in previous studies [32,34-36].

General linear model analysis

Pre-processed data were then analyzed at the group level by means of a general linear model (GLM) for main effects, between-condition contrast analysis, structural equation modeling (SEM), and Region-of-Interest (ROI) Analysis. The group GLM included a set of basis functions consisting of the predicted BOLD response to the stimulation paradigm, based on the stimulus timing convolved with the hemodynamic response function, a constant function, and models of physiological noise. The details of the GLM analysis are provided in supplementary on-line material.

SEM analysis

Structural Equation Modeling was performed separately for each condition to identify significant connections, and how they vary with the study conditions. SEM uses a predefined model of known anatomical connections [37] to investigate multiple simultaneous connections between regions. The underlying concept is that BOLD signal fluctuations in a region are most closely related to input signaling from other regions. The results of the SEM analysis are the linear weighting factors (i.e. β-values) that reflect the connectivity between regions. In order to allow for variations in connectivity between regions over time, SEM was applied in a dynamic sense. Connectivity values were calculated using data from all participants within periods spanning roughly 40 seconds within the stimulation paradigm. This was repeated for all periods in a sliding-window manner. The SEM methods have been extensively validated in previous studies, and the details are provided in Supplementary On-Line Material [38].

ROI analysis

A region-of-interest analysis was performed using the sub-regions that were identified during the SEM analyses. ROIs were assessed in terms of the means and standard deviations of their beta-values as determined via the group GLM analysis. These values were used to compare the neural responses between the Positive, Neutral, and Negative conditions via repeated measures ANOVA. Similar to the GLM analysis, the ROI analysis demonstrates consistent features of the responses across groups and conditions.

Results

Behavioral results

Descriptive statistics for Pain Intensity and Unpleasantness ratings are shown in Table 1. A One-way repeated-measures ANOVA revealed significant differences between conditions, supporting the emotional modulation of pain perception for both pain Intensity, F (1, 20) = 16.251, $p < 0.01$ and Unpleasantness ratings, F (1, 20) = 18.30, $p < 0.01$. Follow-up pair-wise comparisons revealed that pain Intensity ratings were significantly higher for the Negative condition (M = 48.74, SD = 10.60) than the Positive condition (M = 44.22, SD = 10.75; $p <$ 0.01), and were significantly higher for the Neutral con-

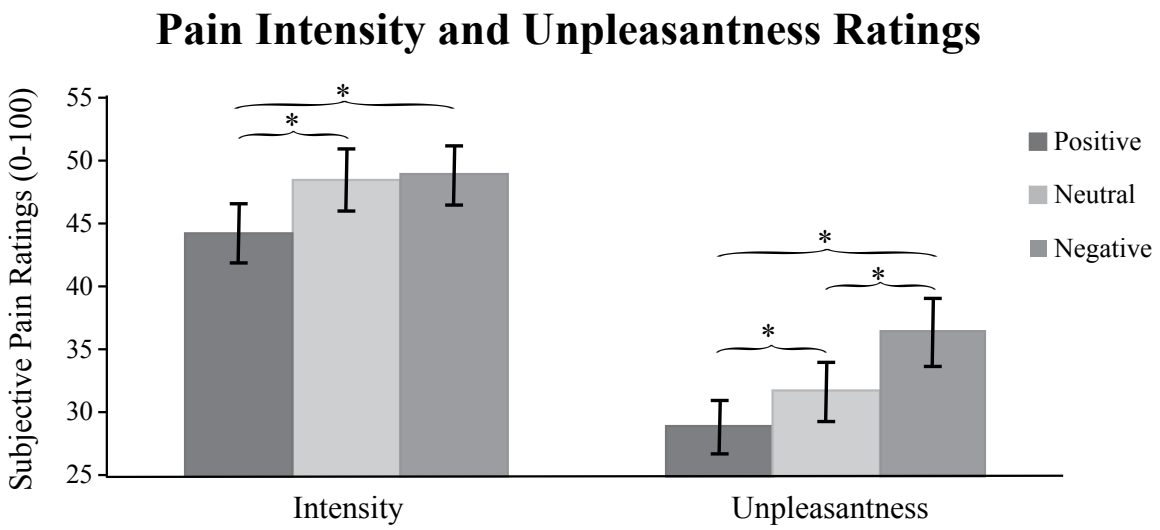

Figure 2: Bar Graph of Average Pain Intensity and Unpleasantness Ratings. A significant difference of $p < 0.05$ is indicated by*.

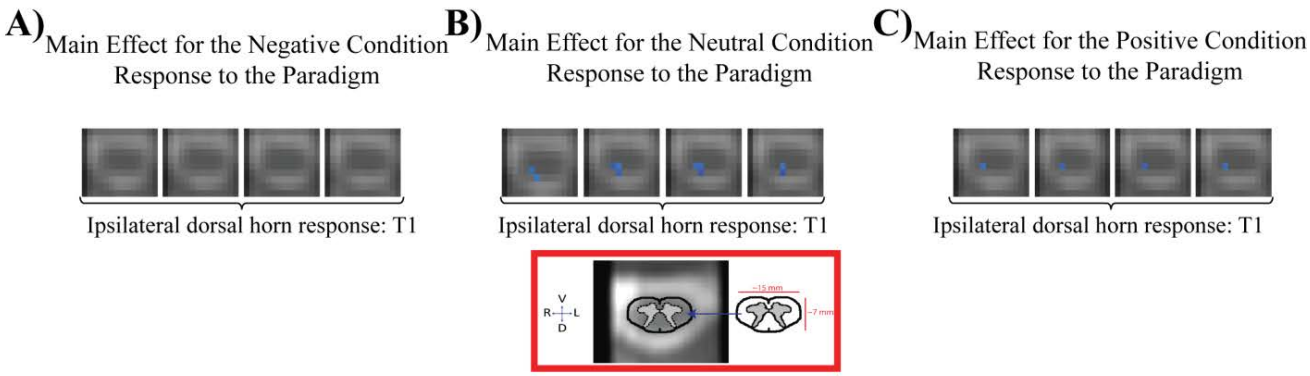

Figure 3: GLM results showing the main effects of the A) Negative, B) Neutral, and C) Positive Conditions. The slices shown are contiguous 1-mm thick axial slices and show the responses from the T1 spinal cord segment. Both the Neutral and Positive conditions reveal significant decreases in BOLD signal in the right dorsal horn of the T1 segment.

Table 1: Descriptive Statistics for Pain Intensity and Unpleasantness Ratings.

	Mean	Median	Standard Deviation
Pain Intensity			
Positive	44.22	40.71	10.75
Neutral	48.40	45.71	11.24
Negative	48.74	47.86	10.60
Pain Unpleasantness			
Positive	29.05	29.29	10.10
Neutral	31.85	33.57	10.30
Negative	36.60	35.00	11.92

dition (M = 48.40, SD = 11.24) than the Positive condition ($p < 0.01$) (Figure 2). There was no significant difference between the pain Intensity ratings in the Negative and Neutral conditions.

The One-way repeated-measures ANOVA for Pain Unpleasantness ratings showed significant differences for all three comparisons (Figure 2). Follow-up pair-wise contrasts revealed that pain Unpleasantness ratings were significantly higher in the Negative condition (M = 36.60, SD = 11.92) than in the Positive (M = 29.05, SD = 10.09; $p < 0.01$) and Neutral (M = 31.85, SD = 10.30; $p < 0.01$) conditions. Pain ratings in the Neutral condition were also significantly higher than those in the Positive condition ($p = 0.04$). All follow-up pair-wise contrasts were Bonferroni corrected for multiple comparisons.

Functional MRI results

Group-level GLM results revealed the significant effect of noxious thermal stimulation compared to baseline (non-noxious thermal stimulation) separately for each of the affective conditions (Supplementary Table 1). These analyses revealed significant BOLD signal decreases ($p < 0.001$) in the right dorsal horn of the first thoracic spinal cord segment (T1) in both the Neutral and Positive conditions, but not the Negative condition (Figure 3). There were no significant BOLD signal changes in the C6 dorsal horn (corresponding to the stimulated dermatome) for any of the three affective conditions.

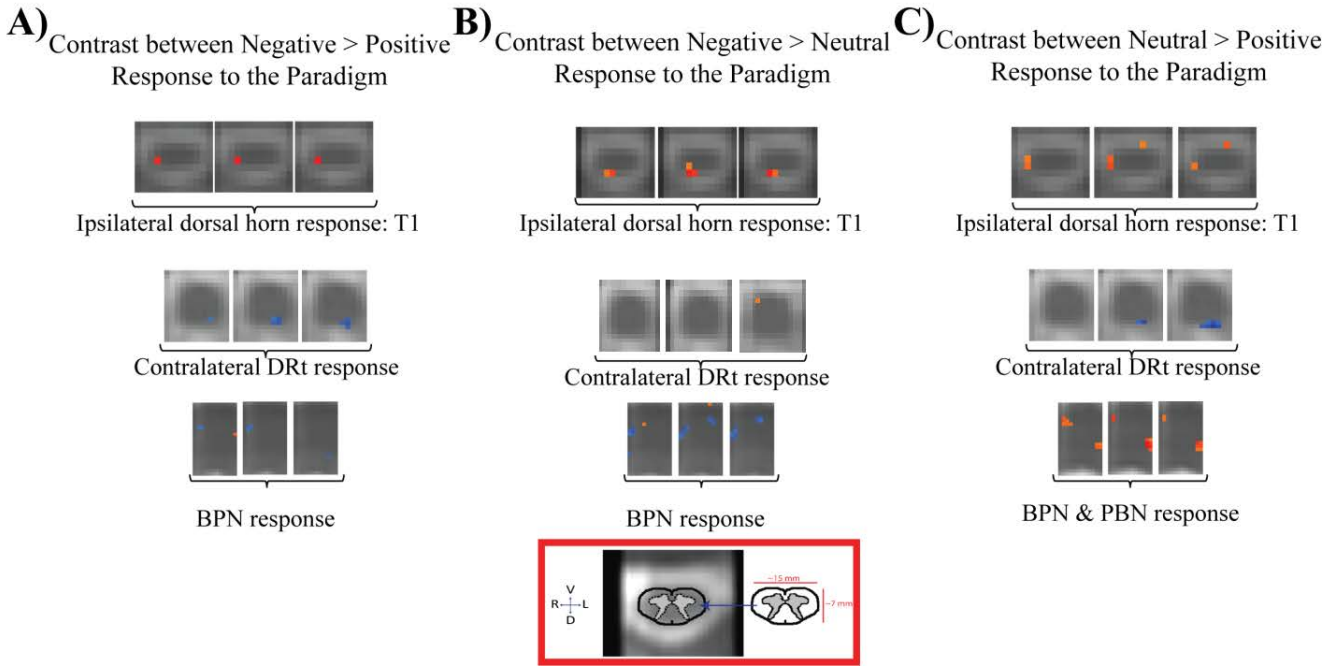

Figure 4: Results of the contrast analysis to compare the BOLD signal changes between the Positive, Neutral, and Negative Conditions. Specific contrasts include A) Negative > Positive, B) Negative > Neutral, and C) Neutral > Positive. Axial slices are displayed at 1st thoracic segment of the spinal cord, the caudal medulla, and at the level of the pons. Warm colors indicate BOLD responses that were greater in the primary condition, while cool colors indicate BOLD responses that were greater in the reverse contrast. Key areas with significantly different responses are shown to be the right dorsal region of the T1 segments near the DRt in the medulla, and in the vicinity of the PBN and BPN in the Pons.

The group-level between-condition contrasts demonstrated several regions in the spinal cord and brainstem that exhibited significant differences in BOLD responses ($p < 0.001$) (Supplementary Table 2). All three contrasts (Negative > Positive, Negative > Neutral, and Neutral > Positive) revealed significant differences in the T1 region of the spinal cord. Consistent with the group GLM results, these contrasts reveal significantly decreased activity in the Positive condition compared to the Neutral and Negative conditions, with decreased responses occurring below the site of stimulation, in the right dorsal horn of the cord at T1, rather than at the level of the stimulated segment (C6) (Figure 4).

At the level of the medulla, there were significantly larger BOLD responses in the Positive condition compared to both the Neutral and Negative conditions in the area of the contralateral DRt. There was no significant difference between the Negative and Neutral conditions in this region. There were also significantly larger BOLD responses for the Neutral condition than both the Negative and Positive conditions at the levels of the Pons in the regions of the parabrachial nucleus (PBN) and basilar pontine nuclei (BPN) of the deep pontine nuclei, with a slightly elevated BOLD response in the region of the BPN for the Positive condition over the Negative condition (Figure 4).

Structural equation modeling results

The SEM analysis was conducted separately the Positive, Neutral, and Negative conditions, and dynamic variations in connectivity were also identified. The best fit results are shown in Figure 5, for periods before, during, and after the application of the noxious thermal stimulus.

It is of note that for all three conditions, connectivity initially observed (before the application of the stimulus) was maintained for the duration of the acquisition. Additional connectivity between regions occurred once the stimulus was applied and again once the stimulus was removed. For example, connectivity of PAG→PBN and C6RD→Thal was maintained throughout the duration of the Negative condition, with the addition of Thal→PAG, PAG→NGc, PAG→NTS, and NTS→PBN during the period when the noxious stimulus was applied, and with the additional recruitment of PBN→NGc, NGc→C6RD, and NTS→C6RD when the stimulus was removed.

Similarly, throughout the Neutral condition, the connectivity of Thal→PAG, Hyp→NGc, PBN→NGc, PBN→NTS, and NTS→C6RD was maintained, connectivity of NTS→PAG, PAG→Hyp, and NGc→C6RD occurred during the period of stimulation and was maintained for the duration, while PAG→NRM and NRM→C6RD connectivity occurred after the noxious stimulus was removed.

Throughout the Positive condition Thal→PAG, NTS→PAG, PBN→NGc, NTS→C6RD, C6RD→NGc,

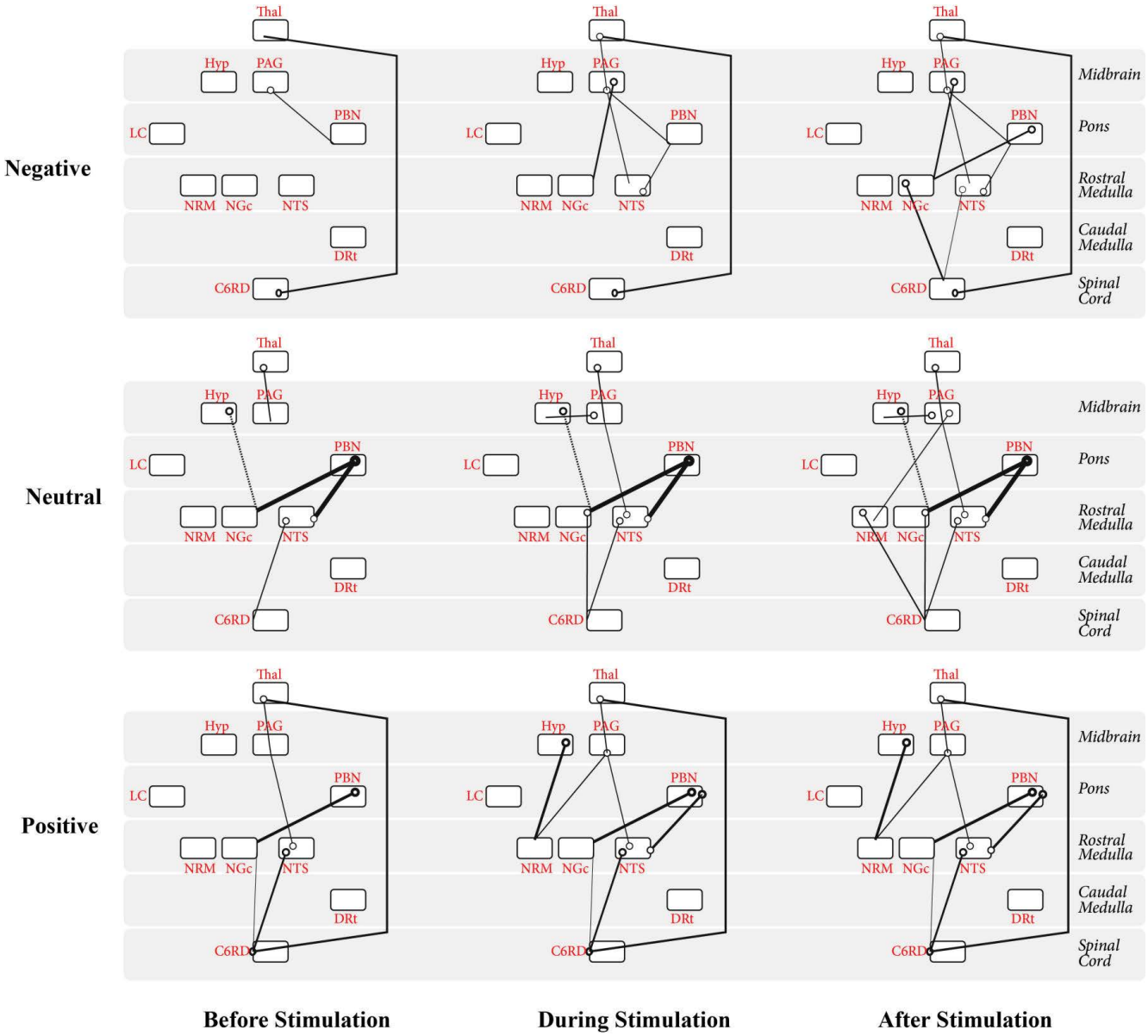

Figure 5: SEM results for the Positive, Neutral, and Negative conditions, before, during, and after the application of the noxious thermal stimulus. Circles indicate the nucleus of the region and directionality of influence, with influence for the connection originating in the nucleus of the specified ROI. The thickness of the lines indicate the strengths of the path coefficients. Solid lines represent positive path coefficients and dashed lines represent the negative coefficients. C6RD = right dorsal region of the C6 spinal cord segment; PBN = Parabrachial Nucleus; LC = Locus Coeruleus; NRM = Nucleus Raphe Magnus; NTS = Nucleus Tractus Solitarius; NGc = Nucleus Gigantocellularis; DRt = Dorsal Reticular Nucleus; PAG = Periaqueductal Gray Matter; Hyp = Hypothalamus; Thal = Thalamus.

Table 2: Average BOLD Percent Signal Change and Relative Standard Error of the Mean, Across Sets, from ROI Analysis.

	Positive	Negative	Neutral
Hypothalamus	-0.06 (± 0.25)	0.27 (± 0.19)	0.18 (± 0.25)
NTS	0.41 (± 0.25)	0.35 (± 0.20)	0.20 (± 0.26)
Thalamus	1.45 (± 1.48)	0.24 (± 0.12)	0.14 (± 0.37)
PAG	0.04 (± 0.16)	0.27 (± 0.20)	0.23 (± 0.27)
LC	0.34 (± 0.24)	0.56 (± 0.24)	0.38 (± 0.29)
PBN	-0.08 (± 0.30)	-0.01 (± 0.31)	-0.11 (± 0.24)
NRM	0.12 (± 0.31)	1.14 (± 0.39)	0.23 (± 0.23)
NGC	-0.29 (± 0.20)	-0.02 (± 0.21)	-0.06 (± 0.23)
DRt	1.00 (± 0.40)	-0.10 (± 0.46)	0.34 (± 0.31)
C6 right dorsal	-0.82 (± 0.42)	-0.40 (± 0.30)	-0.53 (± 0.38)

and C6RD→Thal connectivity was observed. Once the stimulus was applied, additional connectivity of Hyp→NRM, PAG→NRM, and PBN→NTS was observed and maintained for the duration of the acquisition. No additional recruitment occurred following the removal of the noxious stimulus during the Positive condition.

Region-of-interest analysis results

The repeated measures ANOVA for the BOLD responses in selected ROIs showed that only the NRM exhibited significant differences between conditions ($p < 0.05$), with the DRt approaching significance at $p = 0.0713$. There was a linear trend in 7/10 of the ROIs, showing an effect of valence such that the hypothalamus, PAG, LC, NRM, NGC, and the dorsal horn of C6 all exhibited the least increase in BOLD response in the Positive condition and the most in the Negative condition (Table 2), however these differences between conditions only reached significance for the NRM. The DRt showed the opposite trend, with the most increase in BOLD signal occurring for the Positive condition and the least for the Negative, although these differences did not reach significance.

Discussion

The results of this study build on previous research by demonstrating that emotional modulation of pain can be observed using fMRI at the level of the brainstem and spinal cord. The group-level GLM revealed an increased caudal spread of BOLD signal decreases in the ipsilateral dorsal horn at the level of T1, several segments below the level of stimulation, for the Positive and Neutral conditions, but not the Negative condition. This may suggest a decrease in input signaling related to descending pain modulation in the Positive and Neutral condition that was absent from the Negative condition. Group-level between-condition contrast analyses revealed significant differences between conditions at T1 as well. Specifically, the BOLD response was greatest in the Negative condition, comparatively weaker in the Neutral condition, and weaker yet in the Positive condition. The observation of greater relative BOLD signal decrease for the Positive condition is consistent with previous work which found greater BOLD signal decreases in the ipsilateral dorsal horn of the cord when noxious stimulation was paired with music [22]. The present findings are in agreement with Motivational Priming Theory in that the Positive condition seems to render the ipsilateral dorsal horn of the cord less responsive to the noxious stimulus compared to the Neutral and Negative conditions.

Although the noxious thermal stimulus was applied to the thenar eminence, corresponding to innervation of the 6th cervical segment, we did not observe significant group level activations of C6. While unexpected, this outcome may be explained by two different influences: the substantial variability in the overall EMP effect for pain perception, and the significant contributions of descending modulation from higher-level networks. As described in detail in McIver, et al. [25], although emotional modulation of pain perception can be reliably replicated at the group level, strong between-subject variability exists. If the neural response to the noxious stimulus in the ipsilateral dorsal horn of the stimulated segment reflects the variability of EMP perception, this heterogeneity may diminish the main effect of emotion on the BOLD response in this area. Furthermore, it is important to recognize the BOLD response in the dorsal horn reflects a combination of the ascending peripheral input and descending modulation from higher order cortical and subcortical structures. The ipsilateral dorsal horn of C6 was receiving both afferent input from the noxious stimulus as well as descending modulatory input from higher cortical structures. Therefore, although this region of the cord was receiving ample input signaling, it is possible that the net effect of those influences may not have resulted in a significant change in BOLD signal. In contrast, T1 did not receive input from peripheral noxious stimulation, but may have received descending modulatory input from higher cortical structures, such as the DRt and PBN as identified in the between-condition contrasts, resulting in the decrease in neural responsiveness.

Typically recognized for its role in facilitating nociceptive processing [39], the DRt exhibited significantly increased neural response in the Positive condition relative to both the Neutral and Negative conditions. The increased response in this region could reflect an increase in either excitatory or inhibitory presynaptic input [40]. As such, a possible interpretation is that the stronger response for the DRt in the Positive condition relative to the Neutral and Negative conditions may reflect a greater degree of inhibition of its typically pro-nociceptive influences. This would explain the decreased BOLD response observed in more caudal regions of the cord and would correspond with the decreased Intensity and Unpleasantness of pain perceived for the Positive condition relative to the Negative and Neutral conditions.

Greater BOLD responses were observed in the PBN and BPN in the Neutral condition relative to the Positive condition. The BPN also exhibited greater responses in both the Neutral and Positive conditions relative to the Negative condition, although the difference between the Positive and Neutral conditions was notably less pronounced. Critically, while the images viewed during the Positive and Negative conditions were matched for high arousal, the images in the Neutral condition had

low arousal ratings. As such, we postulate that the PBN and BPN could be involved in the emotional modulation of the neural response to pain, specifically in relation to the level of arousal (rather than valence) of the emotional stimulus. The potential for this preferentially arousal-based function of the PBN and BPN is supported by their connections with the amygdala [41-43], which has been found to mediate emotional modulation of autonomic responses based on the arousal, rather than the valence, of emotional stimuli [44]. The PBN is recognized to play a large role in descending pain modulation and in particular, for antinociception [45]. The BPN, while not typically recognized to play a role in descending pain modulation, does, however, receive afferent input from the amygdala and other regions of the limbic system [46]. Its function in emotional modulation of the neural response to pain is therefore more likely rooted in its role in general emotion and arousal processing as compared to an inherent role in descending modulation of pain.

Structural equation modeling results further demonstrated the coordinated influences of regions that are known to be involved with descending pain modulation. A Thal→PAG connection was observed throughout the duration of the stimulation paradigm for all three conditions (with the exception of the period before the onset of stimulation in the Negative condition). Given the consistency across all three conditions, this connection may reflect a neural response to an expectation of a painful experience. The C6RD→Thal connection was present in all stages of the Positive and Negative conditions but was absent in the Neutral condition. That the Positive and Negative conditions share this connection, despite differing in their respective valence, suggests that its involvement may be due to differences in arousal between the neutral and emotion-evoking images. Further insight into the neural processes underlying the effect of arousal on EMP may be gleaned from the connections that are weaker during, or unique to, the Neutral condition as compared to the emotion-evoking conditions. For example, although connectivity between the PBN and NTS or NGc was observed in all conditions, the strength of connectivity between these regions is most pronounced in the Neutral condition. The negatively weighted input of Hyp→NGc is observed solely in the Neutral condition. The results suggest a role for these connections in the processing of high-arousal emotional stimuli relative to their effect on emotional modulation of pain.

Although the two emotion-evoking conditions were found to share SEM commonalities, there were several connections unique to each condition. Of note, during the Positive condition there is Hyp and PAG input to the NRM whereas input to the NRM is absent in the Negative condition, and there is PAG input to the NGc and NTS during the Negative condition that is absent in the Positive condition. NTS input to the spinal cord and PAG is prominent in the Positive, but not Negative, condition. These unique connections for each of the conditions likely reflect the different descending effects of emotional modulation based on the valence of the emotional stimulus. Figure 5 may map the circuitry underlying a continuous component of descending modulation that is modified by emotional cues, and this modulation may influence how people perceive the stimulus when it is applied.

The results of the ROI analysis revealed that the NRM exhibits significant differences between conditions, with the greatest BOLD signal increase for the Negative condition and the least response in the Positive condition. The NRM has been shown to function in both inhibition and facilitation of nociceptive processing [39,47,48]. Although differences in BOLD response between conditions failed to reach significance in the other ROIs, a similar trend supporting the effect of valence was observed in most regions, with the exception of the DRt ROI that showed the reverse trend such that the Positive condition elicited the greatest neural response and the Negative condition elicited the least. This anomalous trend is consistent with the results of the between-condition contrast maps and would support the possible inhibition of the DRt in the effect of emotional modulation on pain neural processing.

Despite advancing our understanding of the neural correlates of descending emotional modulation of pain processing, these finding must be considered in light of certain limitations. First, although we intentionally restricted participant recruitment to females to avoid known sex differences in pain perception and to optimize for the chosen noxious stimulus [16], the current study design does not allow for an examination of potential gender differences in the emotional modulation of pain processing. Similarly, the generalizability of these findings to younger or older samples it not currently clear. Furthermore, emotional modulation of pain perception has been shown to be markedly variable across individuals, and potentially associated with psychological characteristics like depression and anxiety [25]. In addition, it has been shown that the BOLD response to noxious thermal stimulation in the spinal cord and brainstem is correlated with individual levels of pain perception [23]. As such, an important avenue for future research will be to test whether the emotional modulation of pain neural processing in the spinal cord and brainstem reflects different individual-level characteristics.

In conclusion, this study makes significant contributions toward understanding the subcortical neural response involved in emotional modulation of pain. The

results demonstrate a pattern of increased descending modulation, specifically corresponding to greater BOLD signal decreases in the ipsilateral dorsal horn of the cord, for Positive compared to Neutral and Negative emotional modulation of pain. This finding is in accordance with Motivational Priming Theory and demonstrates the influence of the appetitive system to inhibit both the perception and neural processing of noxious stimulation when associated with a positive emotional stimulus. In addition, the valence and arousal of the emotional stimuli differentially affect higher brainstem regions to influence the complexity and strength of the neural networks recruited in the response to emotional modulation of pain.

Acknowledgments

We would like to acknowledge and express our appreciation for assistance in data collection from Emmy Li, Rachael Bosma, Andreea Cotoi, and Roxanne Leung.

Author Contributions

All authors, Dr. Stroman, Dr. Kornelsen, and graduate student Theresa McIver, have contributed substantially to the content of the paper. All three authors contributed to the design of the study. McIver collected and analyzed the data under the supervision of Dr. Stroman. Results were reviewed and interpreted by all three authors. McIver drafted the article, and Dr. Stroman and Dr. Kornelsen reviewed and revised it critically. All authors have given final approval of this manuscript.

References

1. Rhudy JL, Williams AE, McCabe KM, et al. (2005) Affective modulation of nociception at spinal and supraspinal levels. Psychophysiology 42: 579-587.
2. Villemure C, Bushnell MC (2002) Cognitive modulation of pain: how do attention and emotion influence pain processing? Pain 95: 195-199.
3. Villemure C, Slotnick BM, Bushnell MC (2003) Effects of odors on pain perception: deciphering the roles of emotion and attention. Pain 106: 101-108.
4. Zelman DC, Howland EW, Nichols SN, et al. (1991) The effects of induced mood on laboratory pain. Pain 46: 105-111.
5. Weisenberg M, Raz T, Hener T (1998) The influence of film-induced mood on pain perception. Pain 76: 365-375.
6. de Wied M, Verbaten MN (2001) Affective pictures processing, attention, and pain tolerance. Pain 90: 163-172.
7. Smith SD, Kornelsen J (2011) Emotion-dependent responses in spinal cord neurons: a spinal fMRI study. Neuroimage 58: 269-274.
8. Meagher MW, Arnau RC, Rhudy JL (2001) Pain and emotion: effects of affective picture modulation. Psychosom Med 63: 79-90.
9. Rhudy JL, Williams AE, McCabe KM, et al. (2008) Emotional control of nociceptive reactions (ECON): do affective valence and arousal play a role? Pain 136: 250-261.
10. Rhudy JL, Williams AE, McCabe KM, et al. (2006) Emotional modulation of spinal nociception and pain: the impact of predictable noxious stimulation. Pain 126: 221-233.
11. Kenntner-Mabiala R, Pauli P (2005) Affective modulation of brain potentials to painful and nonpainful stimuli. Psychophysiology 42: 559-567.
12. Rainville P, Duncan GH, Price DD, et al. (1997) Pain affect encoded in human anterior cingulate but not somatosensory cortex. Science 277: 968-971.
13. Berna C, Leknes S, Holmes EA, et al. (2010) Induction of Depressed Mood Disrupts Emotion Regulation Neurocircuitry and Enhances Pain Unpleasantness. Biol Psychiatry 67: 1083-1090.
14. Roy M, Piché M, Chen JI, et al. (2009) Cerebral and spinal modulation of pain by emotions. Proc Natl Acad Sci U S A 106: 20900-20905.
15. Villemure C, Laferrière AC, Bushnell MC (2012) The ventral striatum is implicated in the analgesic effect of mood changes. Pain Res Manag 17: 69-74.
16. Feine JS, Bushnell MC, Miron D, et al. (1991) Sex differences in the perception of noxious heat stimuli. Pain 44: 255-262.
17. Wiesenfeld-Hallin Z (2005) Sex differences in pain perception. Gend Med 2: 137-145.
18. Beck A, Steer R, Brown G (1996) Beck Depression Inventory-II. San Antonio, USA, 12-15.
19. Spielberger CD, Gorsuch RL, Lushene R, et al. (1983) Manual for the State-Trait Anxiety Inventory (STAI) (Self Evaluation Questionnaire). Palo Alto, CA: Consulting Psychologist Press.
20. Crowne DP, Marlowe D (1960) A new scale of social desirability independent of psychopathology. J Consult Psychol 24: 349-354.
21. Sullivan MJ, Bishop SR, Pivik J (1995) The pain catastrophizing scale: development and validation. Psychol Assess 7: 524-532.
22. Dobek CE, Beynon ME, Bosma RL, et al. (2014) Music modulation of pain perception and pain-related activity in the brain, brain stem, and spinal cord: a functional magnetic resonance imaging study. J Pain 15: 1057-1068.
23. Khan HS, Stroman PW (2015) Inter-individual differences in pain processing investigated by functional magnetic resonance imaging of the brainstem and spinal cord. Neuroscience 307: 231-241.
24. Stroman PW, Khan HS, Bosma RL, et al. (2016) Changes in pain processing in the spinal cord and brainstem after spinal cord injury characterized by functional magnetic resonance imaging. J Neurotrauma 33: 1450-1460.
25. McIver TA, Kornelsen J, Stroman PW (2018) Diversity in the emotional modulation of pain perception: An account of individual variability. Eur J Pain 22: 319-332.
26. Price DD, Hu JW, Dubner R, et al. (1977) Peripheral suppression of first pain and central summation of second pain evoked by noxious heat pulses. Pain 3: 57-68.

27. Villemure C, Bushnell MC (2009) Mood influences supraspinal pain processing separately from attention. J Neurosci 29: 705-715.

28. Staud R, Craggs JG, Robinson ME, et al. (2007) Brain activity related to temporal summation of C-fiber evoked pain. Pain 129: 130-142.

29. Staud R, Cannon RC, Mauderli, et al. (2003) Temporal summation of pain from mechanical stimulation of muscle tissue in normal controls and subjects with fibromyalgia syndrome. Pain 102: 87-95.

30. Lang PJ, Bradley MM, Cuthbert BN (2008) International affective picture system (IAPS): Affective ratings of pictures and instruction manual. Technical Report A-8. Gainsville, FL: University of Florida.

31. Price DD, McGrath PA, Rafii A, et al. (1983) The validation of visual analogue scales as ratio scale measures for chronic and experimental pain. Pain 17: 45-56.

32. Bosma RL, Stroman PW (2014) Assessment of data acquisition parameters, and analysis techniques for noise reduction in spinal cord fMRI data. Magn Reson Imaging 32: 473-481.

33. Stroman PW, Wheeler-Kingshott C, Bacon M, et al. (2014) The current state-of-the-art of spinal cord imaging: Methods. NeuroImage 84: 1070-1081.

34. Stroman PW, Bosma RL, Cotoi AI, et al. (2016) Continuous Descending Modulation of the Spinal Cord Revealed by Functional MRI. PLoS One 11: e0167317.

35. Bosma RL, Mojarad EA, Leung L, et al. (2016) FMRI of spinal and supra-spinal correlates of temporal pain summation in fibromyalgia patients. Hum Brain Mapp 37: 1349-1360.

36. Bosma RL, Ameli Mojarad E, Leung L, et al. (2015) Neural correlates of temporal summation of second pain in the human brainstem and spinal cord. Hum Brain Mapp 36: 5038-5050.

37. Millan MJ (2002) Descending control of pain. Prog Neurobiol 66: 355-474.

38. Stroman PW (2016) Validation of Structural Equation Modeling Methods for Functional MRI Data Acquired in the Human Brainstem and Spinal Cord. Crit Rev Biomed Eng 44: 227-241.

39. Heinricher MM, Tavares I, Leith JL, et al. (2009) Descending control of nociception: Specificity, recruitment and plasticity. Brain Research Reviews 60: 214-225.

40. Logothetis NK, Pauls J, Augath M, et al. (2001) Neurophysiological investigation of the basis of the fMRI signal. Nature 412: 150-157.

41. Mihailoff GA, Kosinski RJ, Azizi SA, et al. (1989) Survey of noncortical afferent projections to the basilar pontine nuclei:a retrograde tracing study in the rat. J Comp Neurol 282: 617-643.

42. Sarhan M, Pawlowski SA, Barthas F, et al. (2013) BDNF parabrachio-amygdaloid pathway in morphine-induced analgesia. Int J Neuropsychopharmacol 16: 1649-1660.

43. Strobel C, Hunt S, Sullivan R, et al. (2014) Emotional regulation of pain: the role of noradrenaline in the amygdala. Sci China Life Sci 57: 384-390.

44. Wood KH, Ver Hoef LW, Knight DC (2014) The amygdala mediates the emotional modulation of threat-elicited skin conductance response. Emotion 14: 693-700.

45. Willis WD, Westlund KN (1997) Neuroanatomy of the pain system and of the pathways that modulate pain. J Clin Neurophysiol 14: 2-31.

46. Schmahmann JD, Pandya DN (1997) Anatomic organization of the basilar pontine projections from prefrontal cortices in rhesus monkey. J Neurosci 17: 438-458.

47. Porreca F, Ossipov MH, Gebhart GF (2002) Chronic pain and medullary descending facilitation. Trends Neurosci 25: 319-325.

48. Ossipov MH, Dussor GO, Porreca F (2010) Central modulation of pain. J Clin Invest 120: 3779-3787.

Supplementary On-line Material for "Functional MRI Reveals Emotional Modulation of Pain Processing in the Human Cervical Spinal Cord and Brainstem"

Methods

General linear model analysis

The group GLM included a set of basis functions consisting of the predicted BOLD response to the stimulation paradigm, based on the stimulus timing convolved with the hemodynamic response function, a constant function, and the first 2 principal components of the time series data for all voxels in the spinal cord and brainstem. The first two principal components across all voxels account for dominant components of physiological noise (respiration and cardiac effects) and bulk motion and do not include contributions from task-related regressors, which occur within specific localized regions [1-3]. Analyzing the normalized data averaged over the group takes advantage of the fact that signal fluctuations due to random noise and physiological motion that are uncorrelated between acquisitions will be reduced, whereas the consistent BOLD-related fluctuations in signal are synchronized with the stimulus paradigm and will be enhanced [1]. Between-condition contrasts were determined by subtracting the group time series data on a voxel-by-voxel basis. A threshold of $p < 0.001$ was chosen to balance Type-I and Type-II errors-given that the data consisted of approximately 5000 independent voxels, at a p-value threshold of $p < 0.001$, 5 false-positive results (voxels) distributed randomly throughout the analyzed volume, might be expected.

Functional MRI data: preprocessing

Data preprocessing included conversion of the data files from DICOM to NIfTI format, followed by coregistration within each series to correct for bulk motion. Coregistration was carried out in 3D using the nonrigid 3D registration tool in the Medical Image Registration Toolbox (MIRT; [4]). The data were subsequently interpolated to 1 mm cubic voxels and then spatially normalized, in accordance with previously established methods [1,5-7]. The method consists of matching sections of the template to the image data, with a process to ensure that the length of the cord anatomy is not altered compared to the original image data. Fine-tuning normalization is then applied to match the normalized images to the template using the MIRT toolbox [4]. The anatomical reference image was based on data from 356 healthy participants, and a corresponding anatomical region map has been defined as well, as described previously [2,6]. This anatomical map was used to automatically identify anatomical regions in subsequent analyses.

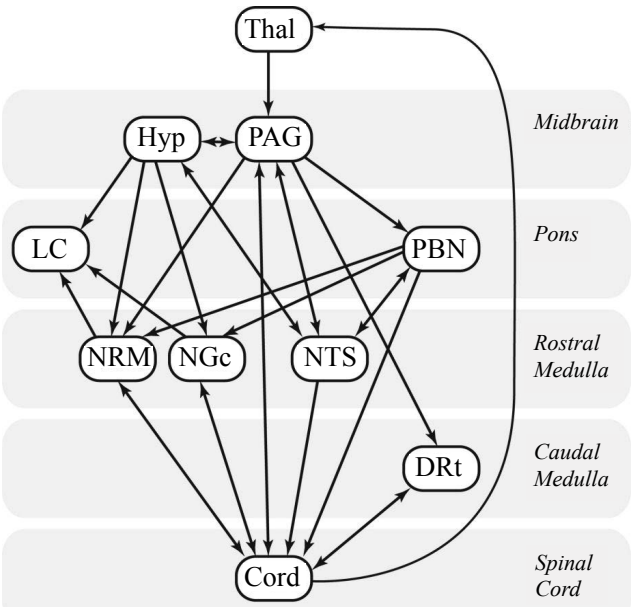

Supplementary Figure 1: The SEM model assumed for analysis; includes the medial portion of the thalamus (Thal), the hypothalamus (Hyp), periaqueductal gray matter (PAG), nucleus raphe magnus (NRM), nucleus gigantocellularis (NGc), parabrachial nucleus (PBN), locus coeruleus (LC), nucleus tractus solitarius (NTS), dorsal reticular nucleus of the medulla (DRt), and right dorsal region of the 6th cervical spinal cord segment (C6 RD).

SEM analysis

The underlying concept is that BOLD signal fluctuations in a region are most closely related to input signaling from other regions. The BOLD signal time-course in a target region is therefore expressed as a weighted sum of the BOLD signal time-courses in the regions that may be providing the input (i.e. the source regions) [8]. The linear weighting factors (β-values) reflect the connectivity between regions. The model assumed for this analysis is shown in Supplementary Figure 1, and includes the medial portion of the thalamus (Thal), the hypothalamus (Hyp), periaqueductal gray matter (PAG), nucleus raphe magnus (NRM), nucleus gigantocellularis (NGc), parabrachial nucleus (PBN), locus coeruleus (LC), nucleus tractus solitarius (NTS), dorsal reticular nucleus of the medulla (DRt), and right dorsal region of the 6th cervical spinal cord segment (C6RD). The anatomical precision of connected regions was also refined by dividing each region in 7 sub-regions based on the BOLD time-course properties, by means of k-means clustering. Networks were investigated for every combination of anatomical sub-divisions of each region in order to identify the

sub-divisions that yielded the best fits to the measured data. In order to allow for variations in connectivity over the course of the stimulation paradigm, SEM analyses were carried out in a dynamic manner. Connectivity values were computed using data only from time periods spanning 40.5 seconds (7 volumes center-to-center), but the time period was shifted one volume at a time, in a sliding-window manner, to span the entire paradigm.

The goodness-of-fit was determined by computing the amount of variance in each target region that is explained by the fit, expressed as the R^2 value. The significance was estimated by converting the R value to a Z-score by means of Fisher's Z-transform. The significance of each network component, with a given set of anatomical sub-divisions, was determined based on previously determined probability distributions [8]. Network components were inferred to be significant at a family-wise error corrected $p_{fwe} < 0.05$. F-tests were used to determine the significance of each source region to the fit to each target region, and significance was inferred at $F(1,\infty) > 3.845$ was used, corresponding to $p < 0.05$. The significance of linear weighting values (i.e. β values) were determined, compared to the null hypothesis (i.e. $\beta = 0$), based on a T-test. Significance was again inferred at a family-wise-error corrected $p_{fwe} < 0.05$, accounting for the total number of network combinations that were tested.

References

1. Bosma RL, Stroman PW (2014) Assessment of data acquisition parameters, and analysis techniques for noise reduction in spinal cord fMRI data. Magn Reson Imaging 32: 473-481.
2. Bosma RL, Ameli Mojarad E, Leung L, et al. (2015) Neural correlates of temporal summation of second pain in the human brainstem and spinal cord. Hum Brain Mapp 36: 5038-5050.
3. Khan HS, Stroman PW (2015) Inter-individual differences in pain processing investigated by functional magnetic resonance imaging of the brainstem and spinal cord. Neuroscience 307: 231-241.
4. Myronenko A, Song X (2010) Intensity-based image registration by minimizing residual complexity. IEEE Trans Med Imaging 29: 1882-1891.
5. Bosma RL, Stroman PW (2015) Spinal cord response to stepwise and block presentation of thermal stimuli: A functional MRI study. J Magn Reson Imaging 41: 1318-1325.
6. Dobek CE, Beynon ME, Bosma RL, et al. (2014) Music modulation of pain perception and pain-related activity in the brain, brainstem, and spinal cord: an fMRI study. J Pain 15: 1057-1068.
7. Stroman PW, Figley CR, Cahill CM (2008) Spatial normalization, bulk motion correction and coregistration for functional magnetic resonance imaging of the human cervical spinal cord and brainstem. Magn Reson Imaging 26: 809-814.
8. Stroman PW (2016) Validation of structural equation modeling methods for functional MRI data acquired in the human brainstem and spinal cord. Crit Rev Biomed Eng 44: 227-241.

Supplementary Table 1: Full list of spinal cord and brainstem regions exhibiting BOLD signal changes in the Group GLM for Main effect of Affective Condition.

		Negative	Neutral	Positive
Spinal Cord Segments				
	C1	2+ Right Dorsal		
		8+ Medial Ventral		
	C2	8+ Right Ventral		
	C3		8- Right Dorsal	
	C4		3- Right Dorsal 10- Right Ventral	
	C5		16- Right Ventral	3- Right Dorsal
	C6	2+ Right Ventral	10+ Left Ventral	2+ Right Ventral
	C7		54+ Left Ventral	15+ Right Ventral
	C8		2+ Left Ventral	
	T1		11- Right Dorsal	4- Right Dorsal
Brainstem				
	Pons	59+ Medial Ventral		
	Medulla	16+ Right Ventral	8+ Left Dorsal	
		8+ Medial Ventral		

Note: All statistical inferences were made at $p < 0.001$. Number of voxels exhibiting BOLD signal increase in a given region is indicated with "+", while BOLD signal decreases are indicated with "-". It is of note that the large extent of ventral activation across the lower spinal cord segments is consistent with Smith SD, et al., who reported a large spread of ventral activity in response to viewing Neutral IAPS images, without any accompanying sensory or motor stimulation.

Supplementary Table 2: Full list of spinal cord and brainstem regions exhibiting differences BOLD response between conditions for the Group-Level Between Condition Contrasts.

		Negative > Positive	Negative > Neutral	Neutral > Positive
Spinal Cord Segments				
	C1	2+ Left Ventral	4- Left Dorsal	
	C2			15- Right Medial
	C3		9+ Right Dorsal	11- Right Ventral 35- Right Dorsal 11- Medial
	C4	3- Medial Ventral	12+ Right Ventral	10- Right Ventral
	C5			
	C6		10- Left Ventral	15+ Left Ventral
	C7	8- Medial Ventral	9- Left Ventral	6- Right Ventral
	C8			
	T1	9+ Right Dorsal	31+ Right Dorsal	15+ Medial Ventral 5+ Right Dorsal
Brainstem				
	Pons	5- Right Ventral (BPN)	13- Right Ventral (BPN)	7+/7- Medial (Caudal)
		13- Left Dorsal	51- Right Ventral	12+ Right Ventral (BPN)
		8+ Medial Ventral	7- Left Ventral	17+ Left Dorsal (PBN)
		5+ Left Medial		24+ Left Ventral (Caudal)
	Medulla	5+ Left Ventral	10+ Right Ventral	18- Left Dorsal (Caudal)
		10- Left Dorsal		12+ Left Dorsal (Rostral)

Note: All statistical inferences were made at $p < 0.001$. Number of voxels exhibiting greater BOLD response in the primary condition is indicated with "+", while "-" indicate BOLD responses that were greater in the reverse contrast.